Inorg. Chem. **2003**, *42*, 1112–1120

Anion Dependent Structures of Luminescent Silver(I) Complexes

Corey Seward, Jacquelyn Chan, Datong Song, and Suning Wang*

Department of Chemistry, Queen's University, Kingston, Ontario K7L 3N6, Canada

Received July 24, 2002

The reaction of AgX, where X = trifluoroacetate ($CF_3CO_2^-$, tfa), nitrate (NO_3^-), trifluoromethanesulfonate (triflate, $CF_3SO_3^-$, OTf), hexafluorophosphate (PF_6^-), or perchlorate (ClO_4^-), with 2,2′,3″-tripyridylamine (tpa) yields five novel silver(I) complexes, which have been structurally characterized. The five complexes have the same 1:1 stoichiometry of Ag/tpa but exhibit different modes of coordination, depending upon the counterion present in the compound. Compound **1**, $[Ag(tpa)(tfa)]_n$, forms a 1D coordination polymer of $[Ag(tpa)(tfa)]_2$ dimer units linked through bridging tfa counterions. Compound **2**, $[Ag(tpa)(CH_3CN)(NO_3)]_n$, forms a zigzag chain 1D coordination polymer exclusively through Ag–N bonds. In compounds **1** and **2**, each tpa ligand is bound to two Ag(I) ions via a 2-py and a 3-py group. Compound **3**, $[Ag(tpa)(OTf)]_n$, forms a ribbonlike 1D coordination polymer, in which each tpa ligand binds to three different silver centers via all three pyridyl groups, and the counterion remains coordinated to the Ag(I) center. Compounds **4**, $[Ag(tpa)(CH_3CN)]_n(PF_6)_n$, and **5**, $[Ag(tpa)(CH_3CN)]_n(ClO_4)_n$, display ribbonlike structures resembling that of **3**, except that the counterions are not coordinated. All complexes are luminescent in acetonitrile solution, with emission maxima in the near-UV region (λ_{max} = 366, 368, 367, 367, and 368 nm for **1**–**5**, respectively). At 77 K, the emission maxima are red-shifted to λ_{max} = 452, 453, 450, 450, and 454 nm for **1**–**5**, respectively.

Introduction

Luminescent compounds are currently of great interest due to their potential applications in chemical sensors, photochemistry, and electroluminescent (EL) displays.[1−3] Blue luminescent compounds are the most sought-after because of the demand for stable blue emitters for EL devices and their potential to function as fluorescent sensors for certain aromatic molecules that absorb in the UV or near UV region. We have demonstrated recently that blue luminescent Zn(II) complexes based on star-shaped di(2-pyridyl)amino, dpa, derivative ligands can selectively detect benzene or toluene molecules.[4] The selectivity and sensitivity of those Zn(II) complexes toward benzene or toluene were found to be highly dependent on the molecular structure and the extended structure of the complex in the solid state. Changing the counterion in the Zn(II) complex has led to the discovery of several structural motifs and a different fluorescent response toward aromatic molecules.[4,5] To further explore the chemistry of blue luminescent compounds and their potential use in sensor technologies, we expanded our investigation to Ag(I) complexes. The Ag(I) ion has a d^{10} electronic configuration like the Zn(II) ion and is not expected to significantly alter the emission color of the luminescent ligand, barring Ag−Ag interactions. However, in contrast to Zn(II), the Ag-

* To whom correspondence should be addressed. E-mail: wangs@chem.queensu.ca.

(1) (a) Tang, C. W.; VanSlyke, S. A. *Appl. Phys. Lett.* **1987**, *51*, 913. (b) Tang, C. W.; VanSlyke, S. A.; Chen, C. H. *J. Appl. Phys.* **1989**, *65*, 3611. (c) Shirota, Y.; Kuwabara, Y.; Inada, H.; Wakimoto, T.; Nakada, H.; Yonemoto, Y.; Kawami, S.; Imai, K. *Appl. Phys. Lett.* **1994**, *65*, 807. (d) Hamada, Y.; Sano, T.; Fujita, M.; Fujii, T.; Nishio, Y.; Shibata, K. *Jpn. J. Appl. Phys.* **1993**, *32*, L514. (e) Bulovic, V.; Gu, G.; Burrows, P. E.; Forrest, S. R. *Nature* **1996**, *380*, 29. (e) Wu, Q.; Esteghamatian, M.; Hu, N.-X.; Popovic, Z. D.; Enright, G.; Tao, Y.; D'Iorio, M.; Wang, S. *Chem. Mater.* **2000**, *12*, 79.

(2) (a) Chassot, L.; Müller, E.; von Zelewsky; A. *Inorg. Chem.* **1984**, *23*, 4249. (b) Vogler, A. Kunkely, H. *Coord. Chem. Rev.* **1998**, *177*, 81. (c) Wan, K. T.; Che, C. M.; Cho, K. C. *J. Chem. Soc., Dalton Trans.* **1991**, 1077. (d). Che, C. M.; Wan, K. T.; He, L. T.; Poon, C. K.; Yam, V. W. W. *J. Chem. Soc., Dalton Trans.* **1989**, 2011. (e) Yersin, H.; Humbs, W.; Strasser, J. *Coord. Chem. Rev.* **1997**, *159*, 325. (f) Paw, W.; Cummings, S. D.; Mansour, M. A.; Connick, W. B.; Gieger, D. K.; Eisenberg, R. *Coord. Chem. Rev.* **1998**, *171*, 125. (g) McGarrah, J. E.; Kim, Y. J.; Hissler, M.; Eisenberg, R. *Inorg. Chem.* **2001**, *40*, 4510.

(3) (a) Kunugi, Y.; Mann, K. R.; Miller, L.; Exstrom, C. L. *J. Am. Chem. Soc.* **1998**, *120*, 589. (b) Song, D.; Wu, Q.; Hook, A.; Kozin, I.; Wang, S. *Organometallics* **2001**, *20*, 4683. (c) Fung, E. Y.; Olmstead, M. M.; Vickery, J. C.; Balch, A. L. *Coord. Chem. Rev.* **1998**, *171*, 151. (d) Vickery, J. C.; Olmstead, M. M.; Fung, E. Y.; Balch, A. L. *Angew. Chem., Int. Ed. Engl.* **1997**, *36*, 1179. (e) De Santis, G.; Fabbrizzi, L.; Licchelli, M.; Poggi, A.; Taglietti, A. *Angew. Chem., Int. Ed. Engl.* **1996**, *35*, 202.

(4) (a) Pang, J.; Marcotte, E. J.-P.; Seward, C.; Brown, R. S.; Wang, S. *Angew. Chem., Int. Ed.* **2001**, *40*, 4042. (b) Seward, C.; Pang, J.; Wang, S. *Eur. J. Inorg. Chem.* **2002**, *6*, 1390.

(5) Mitchell, E.; Seward, C.; Marcotte, E. J. P.; Brown, R. S.; Wang, S. Unpublished results.

10.1021/ic020480q CCC: $25.00
Published on Web 01/24/2003

(I) ion is much larger and has a tendency to display a highly versatile and irregular coordination number and geometry,[6] which may lead to the discovery of new structural motifs and new fluorescent sensors. Previously, we have demonstrated that 2,2′,3″-tripyridylamine (tpa), a dpa derivative, can bind readily to Zn(II) or Ln(III) ions to form luminescent coordination compounds.[7] The Zn(II) complexes of tpa are blue luminescent, attributable to ligand centered emission, while the Ln(III) complexes are either green (Ln = Tb) or red (Ln = Eu) luminescent, attributable to the Ln(III) emission activated by the tpa ligand.[7] The coordination mode of tpa to metal centers in our previously reported Zn(II) and Ln(III) complexes has been exclusively terminal through the 3-pyridyl-nitrogen atom.[7] We have observed that the structures of our new Ag(I) complexes of tpa are in sharp contrast to those of Zn(II) complexes of tpa. Furthermore, we have observed that the structures of the tpa Ag(I) complexes are highly dependent on the counterion.

A number of Ag(I) systems with aromatic, nitrogen-based ligands that exhibit different bonding modes depending upon the reaction conditions have been reported recently.[8] It has also been recently demonstrated that changes in the counterion can have a great effect on the solid-state structures of a series of compounds, often with surprising results.[9] However, systematic studies on structural variations of luminescent Ag(I) complexes are still scarce. We investigated five tpa complexes of silver(I) salts: trifluoroacetate ($CF_3CO_2^-$, tfa^-), nitrate (NO_3^-), and trifluoromethanesulfonate ($CF_3SO_3^-$, triflate, OTf^-), hexafluorophosphate (PF_6^-), and perchlorate (ClO_4^-). These compounds not only display interesting and unusual structural features but also show promise as effective fluorescent sensors toward aromatic molecules. Herein, we report our findings on the luminescent and structural properties of $[Ag(tpa)(tfa)]_n$, **1**, $[Ag(tpa)(NO_3)(CH_3CN)]_n$, **2**, $[Ag(tpa)(OTf)]_n$, **3**, $[Ag(tpa)(CH_3CN)]_n(PF_6)_n$, **4**, and $[Ag(tpa)(CH_3CN)]_n(ClO_4)_n$, **5**. Their use as fluorescent sensors will be reported in due course.

Experimental Section

Silver(I) trifluoroacetate and silver(I) triflate were purchased from Strem, silver(I) nitrate was purchased from Mallinckrodt, silver(I) perchlorate was purchased from BDH, silver(I) hexafluorophosphate was purchased from Aldrich, and solvents were purchased from Fisher. All chemicals and solvents were used without further purification, excepting CH_2Cl_2, which was dried over P_2O_5 where indicated. Perchlorate salts of metal complexes with organic ligands are potentially explosive. In general, when noncoordinating anions are required, every attempt should be made to substitute species such as the fluoro sulfonates for the perchlorates. The tpa ligand was synthesized according to previously published methods.[7] Syntheses of **1, 2**, **4**, and **5** were carried out under air, in a fume hood. Synthesis of **3** was originally carried out under N_2 on a Schlenk line and later repeated in air. All recrystallizations were conducted under air, with vials covered in aluminum foil to prevent decomposition of the silver metal centers due to light exposure. ^{1}H NMR spectra were recorded on Bruker Avance 300 and 400 MHz spectrometers. Elemental analyses were performed by Canadian Microanalytical Service, Ltd., Delta, BC. UV−visible absorption spectra were recorded on a Hewlett-Packard HP8452A diode array spectrophotometer. Excitation and emission spectra were recorded on a Photon Technology International QuantaMaster model C-60 spectrometer, using band pathways of 3 nm for both excitation and emission and presented uncorrected. Lifetime measurements were performed on a Photon Technology International Time Master C-631F spectrometer, using band pathways of 2 nm for both excitation and emission.

Synthesis of 1, $[Ag(tpa)(tfa)]_n$. A sonicated suspension of silver(I) trifluoroacetate (Ag(tfa), 89 mg, 0.403 mmol) in CH_2Cl_2 (5 mL) was added to a solution of tpa (100 mg, 0.403 mmol) in CH_2Cl_2 (5 mL). The mixture was stirred for 1 h, and then, the solvent was removed under reduced pressure. The white powder was partially dissolved in 5 mL of acetonitrile (CH_3CN), filtered, and layered with 5 mL diethyl ether. The vial was covered with aluminum foil and left undisturbed for several days, affording white block crystals of **1** (142 mg, 75%). Elemental analysis calculated for $[Ag(tfa)(tpa)]\cdot H_2O$ (found): C 41.91% (41.74%); H 2.90% (2.29%); N 11.50% (11.10%). ^{1}H NMR data (δ, ppm; CD_3CN, 298 K): 8.37 (dd, J = 4.9 Hz, 1.9 Hz, 1H, H(15)), 8.35 (d, J = 2.7 Hz, 1H, H(11)), 8.28 (ddd, J = 4.9 Hz, 1.9 Hz, 0.8 Hz, 2H, H(5), H(10)), 7.71 (ddd, J = 8.2 Hz, 7.4 Hz, 1.9 Hz, 2H, H(3), H(8)), 7.54 (ddd, J = 8.2 Hz, 2.6 Hz, 1.5 Hz, 1H, H(14)), 7.38 (dd, J = 8.2 Hz, 4.9 Hz, 1H, H(13)), 7.08 (ddd, J = 8.2 Hz, 4.9 Hz, 0.8 Hz, 2H, H(4), H(9)), 7.07 (d, J = 8.2 Hz, 2H, H(2), H(7)). ^{1}H NMR data (δ, ppm; CD_3CN, 233K): 8.28 (ddd, J = 4.8 Hz, 1.9 Hz, 1.2 Hz, 2H, H(5), H(10)), 8.20 (d, J = 2.6 Hz, 1H, H(11)), 8.05 (d, J = 4.8 Hz, 1H, H(15)), 7.76 (ddd, J = 8.3 Hz, 7.3 Hz, 1.8 Hz, 2H, H(3), H(8)), 7.48 (ddd, J = 8.3 Hz, 2.7 Hz, 1.5 Hz, 1H, H(14)), 7.35 (dd, J = 8.3 Hz, 4.9 Hz, 1H, H(13)), 7.15 (ddd, J = 7.3 Hz, 5.0 Hz, 0.9 Hz, 2H, H(4), H(9)), 7.11 (d, J = 8.3 Hz, 2H, H(2), H(7)).

Synthesis of 2, $[Ag(tpa)(NO_3)(CH_3CN)]_n$. A sonicated suspension of silver(I) nitrate (68 mg, 0.403 mmol) in CH_2Cl_2 (4 mL) was added to a solution of tpa (100 mg, 0.403 mmol) in CH_2Cl_2 (5 mL). The mixture was stirred overnight in an aluminum-foil-covered vial. The solvent was removed under reduced pressure and the residue partially dissolved in 5 mL of acetonitrile. The mixture was filtered, layered with 5 mL diethyl ether, and left undisturbed (covered in aluminum foil) for several days, affording crystals (yellow plates) of **2** (122 mg, 66%). Elemental analysis calculated (found): C 44.46% (44.24%); H 3.29% (3.23%); N 18.30% (18.19%). ^{1}H NMR data (δ, ppm; CD_3CN, 298 K): 8.30 (ddd, J = 4.9 Hz, 1.9 Hz, 0.8 Hz, 2H, H(5), H(10)), 8.26 (d, J = 2.3 Hz, 1H, H(11)), 8.24 (d, J = 4.9 Hz, 1H, H(15)), 7.75 (ddd, J = 8.3 Hz, 7.4 Hz, 1.9 Hz, 2H, H(3), H(8)), 7.54 (ddd, J = 8.3 Hz, 2.3 Hz, 1.5 Hz, 1H, H(14)), 7.40 (dd, J = 8.2 Hz, 4.9 Hz, 1H, H(13)), 7.14 (ddd, J = 7.3 Hz, 4.9 Hz, 1.9 Hz, 2H, H(4), H(9)), 7.09 (dd, J = 8.3 Hz, 0.8 Hz, 2H, H(2), H(7)).

Synthesis of 3, $[Ag(tpa)(OTf)]_n$. Under inert atmosphere, a solution of silver(I) trifluoromethanesulfonate (silver triflate, Ag-

(6) Lancashire, R. J. In *Comprehensive Coordination Chemistry*; Wilkison, G.; Gillard, R. D.; McCleverty, J. A., Eds.; Pergamon: Oxford, 1987; Vol. 5, Chapter 54.
(7) (a) Yang, W.; Schmider, H.; Wu, Q.; Zhang, Y.; Wang, S. *Inorg. Chem.* **2000**, *39*, 2397. (b) Yang, W.; Chen, L.; Wang, S. *Inorg. Chem.* **2001**, *40*, 507.
(8) (a) Kang, Y.; Lee, S. S.; Park, K.-M.; Lee, S. H.; Kang, S. O.; Ko, J. *Inorg. Chem.* **2001**, *40*, 7027. (b) Reger, D. L.; Semeniuc, R. F.; Smith, M. D. *Inorg. Chem.* **2001**, *40*, 6545. (c) Caradoc-Davies, P. L.; Hanton, L. R.; Henderson, W. *J. Chem. Soc., Dalton Trans.* **2001**, 2749.
(9) (a) Johnson, B. J. S.; Schroden, R. C.; Zhu, C.; Stein, A. *Inorg. Chem.* **2001**, *40*, 5972. (b) Gable, R. W.; Hoskins, B. F.; Robson, R. *J. Chem. Soc., Chem. Commun.* **1990**, 1677. (c) Subramanian, S.; Zaworotko, M. J. *Angew. Chem., Int. Ed. Engl.* **1995**, *34*, 2127. (d) Keegan, J.; Kruger, P. E.; Nieuwenhuyzen, M.; O'Brien, J.; Martin, N. *Chem. Commun.* **2001**, 2192. (e) Melcer, N. J.; Enright, G. D.; Ripmeester, J. A.; Shimizu, G. K. H. *Inorg. Chem.* **2001**, *40*, 4641.

Table 1. Crystallographic Data

	1	2	3	4	5
formula	$C_{17}H_{12}AgF_3N_4O_2$	$C_{17}H_{15}AgN_6O_3$	$C_{16}H_{12}AgF_3N_4O_3S$	$C_{17}H_{15}AgF_6N_5P$	$C_{17}H_{15}AgClN_5O_4$
fw	469.18	459.22	505.23	542.18	496.66
space group	$P2_1/c$	$P2_1/c$	$P2_1/c$	*Pbca*	*Pbca*
a, Å	9.0840(16)	13.334(4)	10.978(4)	6.4389(14)	6.4275(12)
b, Å	21.921(4)	15.668(4)	26.051(10)	23.574(5)	23.160(5)
c, Å	8.7269(17)	9.031(2)	6.444(2)	25.400(5)	24.887(5)
α, deg	90	90	90	90	90
β, deg	94.952(4)	106.232(5)	100.546(7)	90	90
γ, deg	90	90	90	90	90
V, Å^3	1731.3(6)	1811.7(9)	1811.7(11)	3855.5(14)	3704.8(13)
Z	4	4	4	8	8
D_{calcd}, g·cm^{-3}	1.800	1.684	1.852	1.868	1.781
T, K	296	296	296	296	296
μ, cm^{-1}	12.15	11.44	12.84	12.00	12.68
$2\theta_{max}$, deg	56.56	56.64	56.76	56.58	56.92
reflns measured	12471	12899	12861	25738	25112
reflns used (R_{int})	4106 (0.0412)	4297 (0.0329)	4138 (0.1157)	4637 (0.0676)	4528 (0.1354)
params	319	244	248	271	289
final *R* values [$I > 2\sigma(I)$] R1,[a] wR2[b]	0.0293, 0.0360	0.0296, 0.0519	0.1271, 0.3012	0.0553, 0.1952	0.0525, 0.1013
R values (all data) R1,[a] wR2[b]	0.0810, 0.0425	0.0732, 0.0597	0.2644, 0.3613	0.0712, 0.2062	0.2281, 0.1382
GOF on F^2	0.778	0.831	0.893	1.444	0.794

[a] $R1 = \sum||F_o| - |F_c||/\sum|F_o|$. [b] $wR2 = [\sum w[(F_o^2 - F_c^2)^2]/\sum[w(F_o^2)^2]]^{1/2}$. $w = 1/[\sigma^2(F_o^2) + (0.075P)^2]$, where $P = [\mathrm{Max}(F_o^2,0) + 2F_c^2]/3$.

(OTf), 104 mg, 0.403 mmol) in dry CH_2Cl_2 (5 mL) was added via cannula to a solution of tpa (100 mg. 0.403 mmol) in dry CH_2Cl_2 and stirred for 1 h. The solvent was removed under vacuum, and the white powder was partially dissolved in 5 mL of acetonitrile (in air). The mixture was filtered, layered with 5 mL diethyl ether, covered in aluminum foil, and left undisturbed for several days, affording crystals (white needles) of **3** (148 mg, 73%). The synthesis was later successfully repeated in air. Elemental analysis calculated (found): C 38.04% (37.84%); H 2.39% (2.34%); N 11.09% (11.07%). ^{1}H NMR data (δ, ppm; CD_3CN, 298 K): 8.36 (dd, J = 4.8 Hz, 1.5 Hz, 1H, H(15)), 8.34 (d, J = 2.7 Hz, 1H, H(11)), 8.28 (ddd, J = 4.9 Hz, 1.9 Hz, 0.8 Hz, 2H, H(5), H(10)), 7.71 (ddd, J = 8.2 Hz, 7.4 Hz, 1.9 Hz, 2H, H(3), H(8)), 7.54 (m, 1H, H(14)), 7.39 (dd, J = 8.2 Hz, 4.7 Hz, 1H, H(13)), 7.09 (m, 2H, H(4), H(9)), 7.07 (d, J = 8.2 Hz, 2H, H(2), H(7)).

Synthesis of 4, $[Ag(tpa)(CH_3CN)]_n(PF_6)_n$. A solution of tpa (100 mg, 0.403 mmol) in CH_2Cl_2 (4 mL) was added to a suspension of silver(I) hexafluorophosphate ($AgPF_6$, 102 mg, 0.403 mmol) in CH_2Cl_2 (6 mL). The mixture was stirred overnight, in an aluminum-foil-covered vial. The solvent was then removed under reduced pressure, and the residue was partially dissolved in 5 mL of acetonitrile. The mixture was filtered, layered with 5 mL diethyl ether, and left, covered in aluminum foil, for several days, yielding white block crystals of **4** (113 mg, 52%). Elemental analysis calculated (found): C 37.66% (37.05%); H 2.79% (2.75%); N 12.92% (12.41%). ^{1}H NMR data (δ, ppm; CD_3CN, 298 K): 8.35 (dd, J = 5.0 Hz, 1.6 Hz, 1H, H(15)), 8.34 (d, J = 3.0 Hz, 1H, H(11)), 8.28 (ddd, J = 4.9 Hz, 1.9 Hz, 0.8 Hz, 2H, H(5), H(10)), 7.72 (ddd, J = 8.2 Hz, 7.4 Hz, 1.9 Hz, 2H, H(3), H(8)), 7.54 (ddd, J = 8.2 Hz, 2.6 Hz, 1.5 Hz, 1H, H(14)), 7.39 (ddd, J = 8.2 Hz, 4.8 Hz, 0.6 Hz, 1H, H(13)), 7.09 (ddd, J = 8.2 Hz, 4.9 Hz, 0.8 Hz, 2H, H(4), H(9)), 7.08 (d, J = 8.5 Hz, 2H, H(2), H(7)).

Synthesis of 5, $[Ag(tpa)(CH_3CN)]_n(ClO_4)_n$. A solution of tpa (100 mg, 0.403 mmol) in CH_2Cl_2 (4 mL) was added to a suspension of silver(I) perchlorate ($AgClO_4$, 83.5 mg, 0.403 mmol) in CH_2Cl_2 (6 mL). The mixture was stirred overnight, in an aluminum-foil-covered vial. The solvent was then removed under reduced pressure, and the residue was partially dissolved in 5 mL of acetonitrile. The mixture was filtered, layered with 5 mL diethyl ether, and left undisturbed for several days (covered in aluminum foil), affording white needle crystals of **5** (73 mg, 36%). Elemental analysis calculated (found): C 41.11% (39.91%); H 3.04% (2.82%); N 14.10% (13.02%). Subsequent analyses performed after 3 days gave C 38.46%, H 2.74%, N 12.46%, indicating that the compound decomposes over time. ^{1}H NMR data (δ, ppm; CD_3CN, 298 K): 8.34 (dd, J = 4.9 Hz, 1.4 Hz, 1H, H(15)), 8.32 (d, J = 2.6 Hz, 1H, H(11)), 8.28 (ddd, J = 4.9 Hz, 1.9 Hz, 0.8 Hz, 2H, H(5), H(10)), 7.72 (ddd, J = 8.2 Hz, 7.4 Hz, 1.9 Hz, 2H, H(3), H(8)), 7.55 (ddd, J = 8.2 Hz, 2.6 Hz, 1.5 Hz, 1H, H(14)), 7.39 (dd, J = 8.2 Hz, 4.8 Hz, 1H, H(13)), 7.10 (ddd, J = 7.3 Hz, 4.9 Hz, 0.8 Hz, 2H, H(4), H(9)), 7.08 (d, J = 8.2 Hz, 2H, H(2), H(7)).

X-ray Crystallographic Analysis. All crystals were obtained from acetonitrile/diethyl ether solutions and were mounted on glass fibers. All data were collected on a Bruker SMART CCD 1000 X-ray diffractometer with graphite-monochromated Mo Kα radiation, operating at 50 kV and 30 mA at 23 °C. Data were collected over 2θ ranges 3.72−56.56°, 4.10−56.64°, 3.02−56.76°, 1.73−28.29°, and 1.64−28.46°, for **1**−**5**, respectively. No significant decay was observed during the data collection. Data were processed on a Pentium PC using the Bruker AXS Windows NT SHELXTL software package (version 5.10).[10] Neutral atom scattering factors were taken from Cromer and Waber.[11] Crystals of **1**, **2**, and **3** belong to the monoclinic space group $P2_1/c$, while crystals of **4** and **5** belong to the orthorhombic space group *Pbca*, uniquely determined by systematic absences. All structures were solved by direct methods. The CF_3 group in **1** displays a pseudo-2-fold rotational disorder, which was refined successfully. The *R*-values for the crystal of **3** are high because the crystal was twinned, and the reflections had to be manually separated. The high residual electron peak in **3** (5.300 e/Å^3) is closely associated with the silver atom, and its magnitude is also an artifact of the twinned crystal. The perchlorate counterion in **5** displays some vibrational disorder, which was refined successfully. All non-hydrogen atoms were refined anisotropically, the positions for all hydrogen atoms were calculated, and their contributions were included in the structure factor calculations. Crystallographic data are given in Table 1, and

(10) *SHELXTL NT Crystal Structure Analysis Package*, Version 5.10; Bruker AXS, Analytical X-ray System: Madison, WI, 1999.
(11) Cromer, D. T.; Waber, J. T. *International Tables for X-ray Crystallography*; Kynoch Press: Birmingham, U.K., 1974; Vol. 4, Table 2.2A.

Table 2. Selected Bond Lengths (Å) and Angles (deg) for Compounds **1**−**5**

	Compound **1**		
Ag(1)−N(3)′	2.2417(19)	Ag(1)−O(2)	2.590(2)
Ag(1)−N(1)	2.254(2)	Ag(1)−O(1)	2.642(2)
Ag(1)−O(2)′	2.687(2)		
N(3)′−Ag(1)−N(1)	143.89(8)	C(16)−O(2)−Ag(1)	91.75(18)
N(3)′−Ag(1)−O(2)	119.88(8)	C(16)−O(1)−Ag(1)	89.11(20)
N(1)−Ag(1)−O(2)	95.60(7)		
	Compound **2**		
Ag(1)−N(1)	2.294(2)	Ag(1)−N(6)	2.381(3)
Ag(1)−N(3)′	2.310(2)	Ag(1)−O(1)	2.590(3)
Ag(1)−O(2)	2.633(3)		
N(1)−Ag(1)−N(3)′	116.08(7)	N(1)−Ag(1)−O(1)	109.43(7)
N(1)−Ag(1)−N(6)	118.90(9)	N(3)′−Ag(1)−O(1)	91.72(8)
N(3)′−Ag(1)−N(6)	98.83(9)	N(6)−Ag(1)−O(1)	118.30(9)
N(5)−O(2)−Ag(1)	96.4(2)	N(5)−O(1)−Ag(1)	98.4(2)
C(16)−N(6)−Ag(1)	172.1(3)		
	Compound **3**		
Ag(1)−N(3)′	2.238(13)	Ag(1)−O(1)	2.509(12)
Ag(1)−N(1)	2.299(13)	Ag(1)−N(2)′	2.588(15)
N(3)′−Ag(1)−N(1)	149.6(4)	N(1)−Ag(1)−N(2)′	86.5(5)
N(3)′−Ag(1)−O(1)	115.7(5)	O(1)−Ag(1)−N(2)′	122.6(4)
N(1)−Ag(1)−O(1)	88.2(4)	S(1)−O(1)−Ag(1)	117.4(7)
N(3)′−Ag(1)−N(2)′	94.8(5)		
	Compound **4**		
Ag(1)−N(3)′	2.218(3)	Ag(1)−N(1)	2.356(3)
Ag(1)−N(2)′	2.342(4)	Ag(1)−N(5)	2.748(6)
N(3)′−Ag(1)−N(2)′	140.36(12)	N(3)′−Ag(1)−N(1)	124.97(11)
N(2)′−Ag(1)−N(1)	91.63(12)	N(3)′−Ag(1)−N(5)	85.69(15)
N(5)−Ag(1)−N(1)	118.78(17)	N(5)−Ag(1)−N(2)′	89.25(16)
N(5)−Ag(1)−C(16)	158.1(7)		
	Compound **5**		
Ag(1)−N(3)′	2.216(6)	Ag(1)−N(1)	2.346(6)
Ag(1)−N(2)′	2.316(6)	Ag(1)−N(5)	2.865(10)
N(3)′−Ag(1)−N(2)′	138.8(2)	N(3)′−Ag(1)−N(1)	124.4(2)
N(2)′−Ag(1)−N(1)	94.2(2)	N(5)−Ag(1)−N(1)	116.4(3)
N(5)−Ag(1)−N(3)′	87.6(3)	N(5)−Ag(1)−N(2)′	87.2(3)
Ag(1)−N(5)−C(16)	159.1(17)		

selected bond lengths and angles are given in Table 2.

Results and Discussion

Syntheses and Crystal Structures. (a) tpa. The tpa ligand was synthesized by using Ullmann condensation methods as reported previously.[7] The Ag(I) complexes were obtained by using a 1:1 ratio of Ag(I) salt versus the tpa ligand in CH_2Cl_2, followed by recrystallization from CH_3CN/diethyl ether in moderate to good yields. The structures of compounds **1**−**5** were examined by a single-crystal X-ray diffraction analysis. As shown in Figures 1−5, none of the tpa ligands are planar; instead, they adopt a propeller-like arrangement. The central nitrogen atom, N(4), in each of the complexes is coplanar with the three carbon atoms to which it is bonded, C(1), C(6), and C(12). The average dihedral angles between the pyridyl ring planes and the NC_3 plane are 38.6°, 41.8°, 40.3°, 42.7°, and 44.4°, for **1**−**5**, respectively. These are similar to the crystal structure of the free tpa ligand,[7] which has an average dihedral angle of 38.6°. We did not observe any chelation mode by the tpa ligand in any of the complex structures **1**−**5**. This observation may be partially attributed to the bite angle of the 2,2′-dipyridylamine functionality in tpa. In the structure of a related compound, Zn(2, 2′,2″-tpa)Cl_2, where two of the pyridyl groups are chelated to a zinc(II) center, the six-membered metallocycle formed by the chelate is quite strained.[7] Because silver(I) is a larger cation than zinc(II), there would be more steric strain in a chelated system, which perhaps plays a role in the absence of a tpa chelate mode in compounds **1**−**5**. The three bridging bonding modes displayed by tpa in compounds **1**−**5** are represented in Scheme 1. In bonding mode a, the tpa functions as a bridging ligand via a 2-py and the 3-py group, to form a dinuclear unit. In bonding mode b, the tpa again functions as a bridging ligand via a 2-py and the 3-py group to form an extended 1D chain. In bonding mode c, the tpa functions as a bridging ligand through all three pyridyl groups, leading to the formation of a 1D ribbon structure.

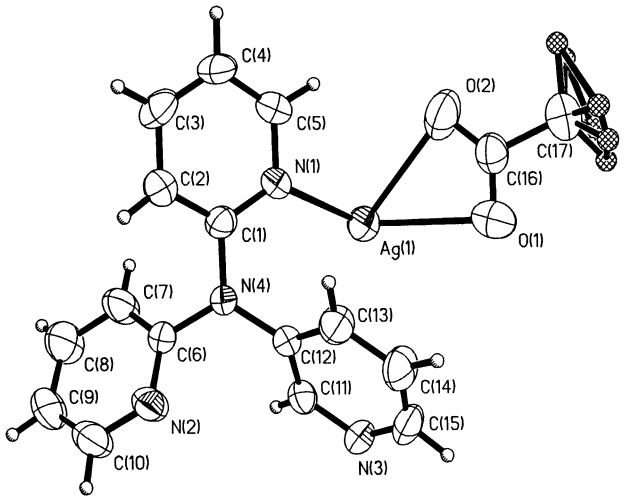

Figure 1. ORTEP diagram showing the unique portion of **1** with 50% thermal ellipsoids and the labeling scheme. The disordered fluorine atoms are not labeled.

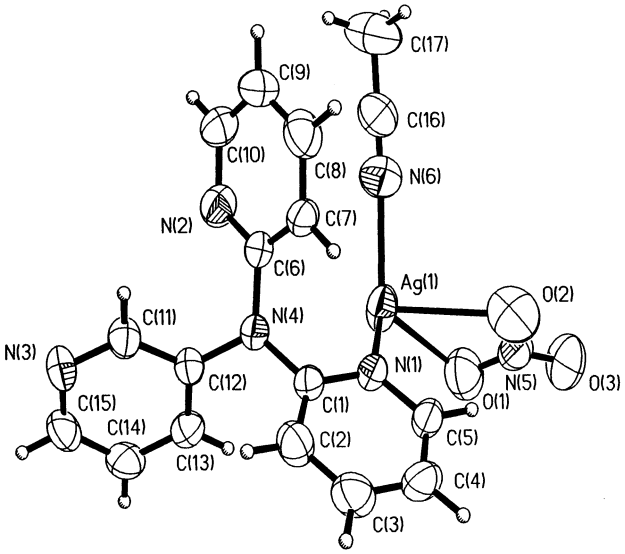

Figure 2. ORTEP diagram showing the unique portion of **2** with 50% thermal ellipsoids and the labeling scheme.

(b) Coordination. At first glance, compound **1** appeared to be a simple dinuclear compound with the formula [Ag(tpa)(tfa)]$_2$. The tpa ligand bridges two Ag(I) ions with typical

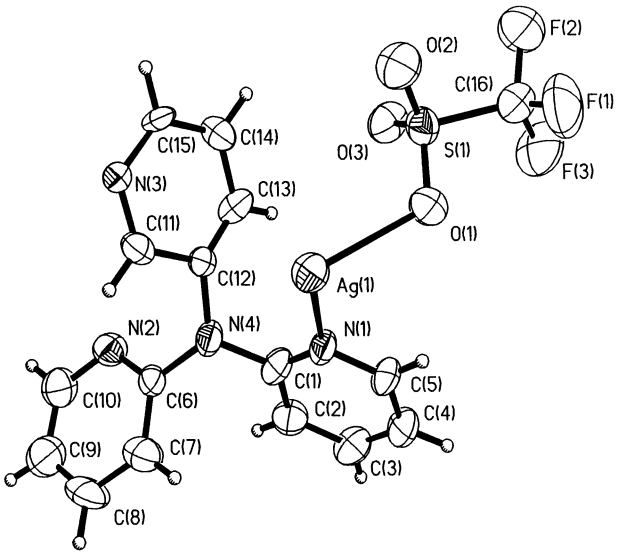

Figure 3. ORTEP diagram showing the unique portion of **3** with 50% thermal ellipsoids and the labeling scheme.

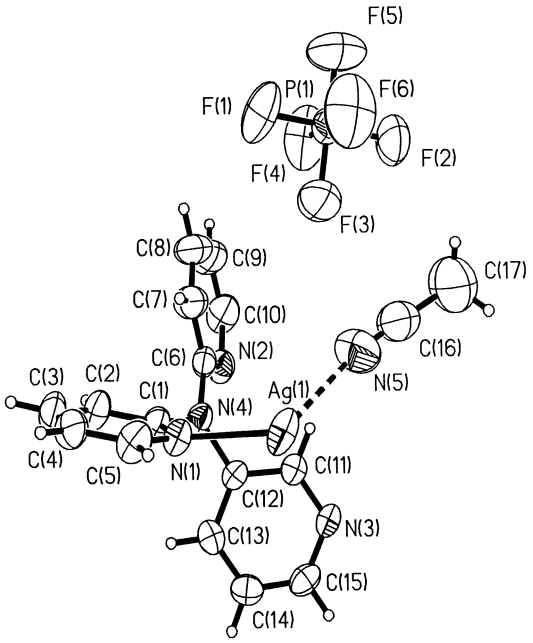

Figure 4. ORTEP diagram showing the unique portion of **4** with 50% thermal ellipsoids and the labeling scheme.

Ag−N bond lengths[6,8] through the N(1) and N(3) pyridyl rings (bonding mode a), in an inward-facing (*endo*) fashion, while the remaining pyridyl ring, containing N(2), does not participate in any coordination (Figures 1 and 6). The trifluoroacetate anion functions as a chelate ligand to the silver center. Upon closer examination of the structure, it became apparent that the trifluoroacetate ligand functions not only as a chelate ligand but also as a bridging ligand via one of oxygen atoms (O(2)) to a silver(I) ion in the neighboring dimer unit, thus linking the dimer units together to form a 1D coordination polymer (Figure 7). The steric demands of the chelating and bridging modes of bonding displayed by the tfa counterion are likely responsible for the binding of only two of the three available tpa pyridyl rings. The Ag−O bond distances are somewhat long but are within

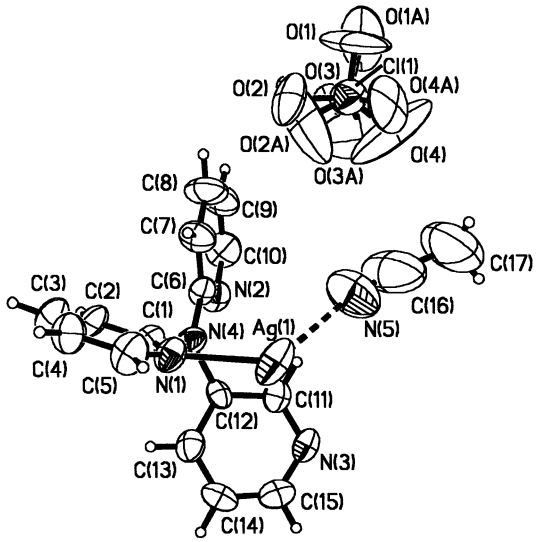

Figure 5. ORTEP diagram showing the unique portion of **5** with 50% thermal ellipsoids and the atom labeling scheme.

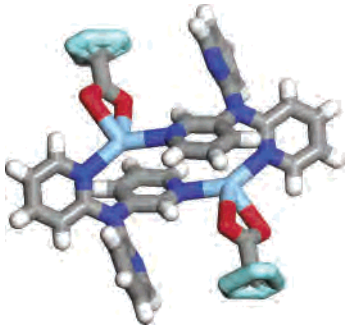

Figure 6. Dimer unit in **1**. Red, oxygen; dark blue, nitrogen; light blue, silver; turquoise, fluorine.

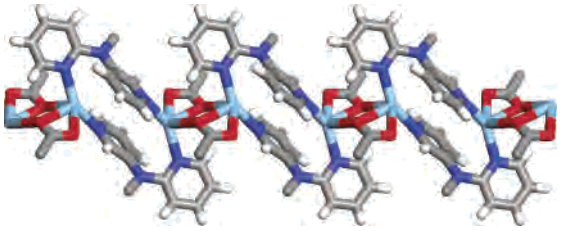

Figure 7. Chain structure of **1**. Noncoordinating pyridyl groups and disordered fluorines have been removed for clarity.

the typical Ag−O bond lengths previously reported.[6] Similar bonding modes displayed by carboxylates have been observed previously.[12] The Ag(I) center in **1** is five-coordinate with an irregular geometry.

Although the anion is different in compound **2**, chelation by the counterion nitrate in a similar manner as the tfa ligand in **1** was again observed. However, unlike the tfa anion, the nitrate anion in **2** does not display a bridging mode (Figure 2). The tpa ligand in **2** functions again as a bridging ligand through one 2-pyridyl- and one 3-pyridyl-nitrogen atom with Ag−N bond lengths similar to those of **1**. However, instead of the *endo* bridging conformation as observed in **1** that led to the formation of a dimer structure, the tpa ligand in **2**

(12) Sanchis, M. J.; Gomez-Romero, P.; Folgado, J. V.; Sapina, F.; Ibanez, R.; Beltran, A.; Garcia, J.; Beltran, D. *Inorg. Chem.* **1992**, *31*, 2915.

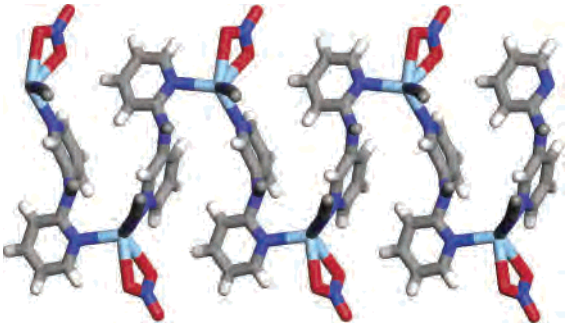

Figure 8. View of the 1D chain of **2**. Noncoordinating pyridyl groups and CH_3CN hydrogens have been removed for clarity.

Scheme 1

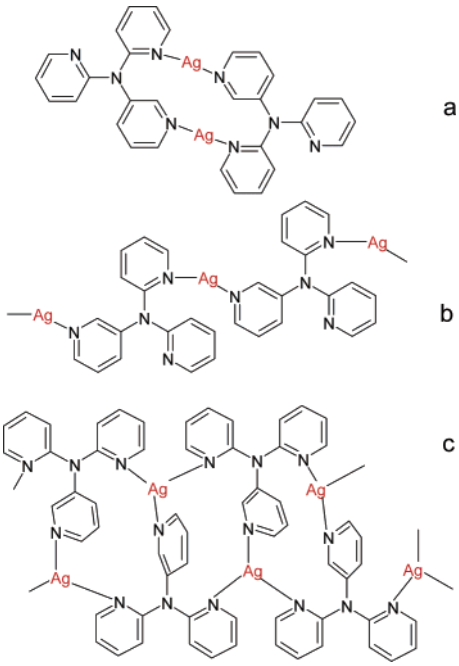

adopts an *exo* bridging conformation, resulting in the formation of a zigzag 1D chain polymer (bonding mode b, Figure 8). Again, one of the 2-pyridyl rings does not participate in coordination, and the Ag(I) center is five-coordinate with an irregular geometry. Because the counterion is no longer bridging between two metal centers, an additional ligand is required to fill the fifth coordination site, which is achieved by an acetonitrile solvent molecule. The CH_3CN presumably coordinates as a means of creating better solid-state packing. Because the syntheses and crystallizations of **1** and **2** were carried out under the same conditions and using the same solvent, the structural difference between **1** and **2** can be attributed entirely to the different bonding modes of the nitrate and the tfa anions.

Changing the counterion to triflate, in compound **3**, causes a structural change again. Because triflate usually functions as a noncoordinating counterion in the same manner as a perchlorate,[13] we expected the triflate to simply balance the charge in the lattice, without coordinating to the metal center. However, the crystal structure revealed that it does coordinate

(13) Desiraju, G. R. *Crystal Engineering: The Design of Organic Solids*; Elsevier: New York, 1989.

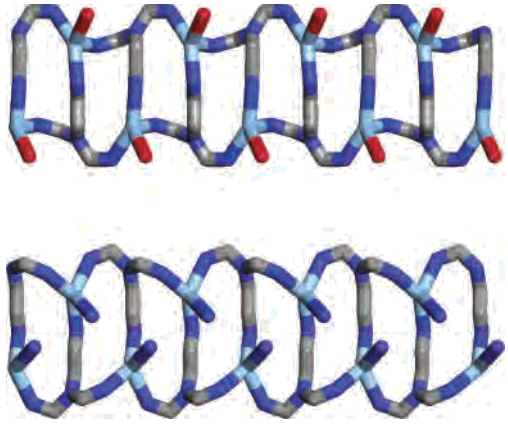

Figure 9. Top: view of the 1D ribbon structure of **3**. Bottom: view of the 1D ribbon structure of **4** and **5**. Atoms not coordinated or part of the backbone have been omitted for clarity.

to the silver center as a terminal ligand and, in fact, forms a shorter bond to the metal center than either the nitrate or trifluoroacetate ligand (Figure 3, see Ag−O distances in Table 2). Although it is rare to observe the coordination of triflate, several examples have been reported previously.[14] In this structure, we finally observed the rare η^3-bridging mode displayed by the tpa ligand (bonding mode c). Each of the pyridyl nitrogen atoms in the tpa ligand forms a bond with one Ag(I) ion. Two of the Ag−N bond lengths are comparable to those of **1** and **2**. However, the third Ag−N bond length is much longer than those of **1** and **2**, most likely caused by steric interactions between ligands due to the crowded coordination sphere around the Ag(I) ion. The lack of chelation from the triflate counterion appears to leave more room around the metal center, allowing the third pyridyl group of the tpa ligand to coordinate and complete the coordination sphere of the Ag(I) ion. The Ag(I) center in **3** is four-coordinate with a distorted tetrahedral geometry. Because of the triple bridge by the tpa ligand, compound **3** forms an interesting ribbon- or ladderlike 1D coordination polymer (Figure 9).

By using either hexafluorophosphate or perchlorate as the counterion for the silver complex, in compounds **4** and **5**, two structures in which the anion is not coordinated to the metal center were achieved (Figures 4 and 5). The crystal structures of compounds **4** and **5** are essentially identical with similar unit cell parameters. The tpa ligand in **4** and **5** again coordinates to three different silver metal centers in the same manner as in **3** (Figure 9). A weakly bound acetonitrile solvent molecule (Ag−N(5) 2.749(6) and 2.836(10) Å, for **4** and **5**, respectively) is present in **4** and **5**, apparently to complete the coordination sphere of the Ag(I) ion. In contrast to the structure of **3**, where one of the pyridyl groups forms a long bond with the Ag(I) ion, the three Ag(I)−N (pyridyl) bonds are similar and comparable to those of **1** and **2**. This can be attributed to the weak Ag(I)−N (CH_3CN) bond and

(14) (a) Makinen, S. K.; Melcer, N. J.; Parvez, M.; Shimizu, G. K. H. *Chem. Eur. J.* **2001**, *7*, 5176. (b) Smith, G.; Cloutt, B. A.; Lynch, D. E.; Byriel, K. A.; Kennard, C. H. L. *Inorg. Chem.* **1998**, *37*, 3236. (c) Kulynych, A. D.;. Shimizu, G. K. H. *CrystEngComm* **2002**, *4*, 102. (d) Yu, J. O.; Cote, A. P.; Enright, G. D.; Shimizu, G. K. H. *Inorg. Chem.* **2001**, *40*, 582.

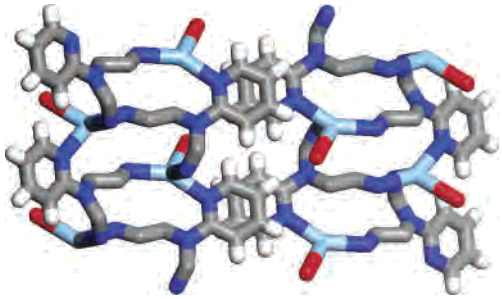

Figure 10. View of **3** showing interchain π-stacking. Only the backbone atoms and the involved pyridyl rings are shown for clarity. The chains extend vertically.

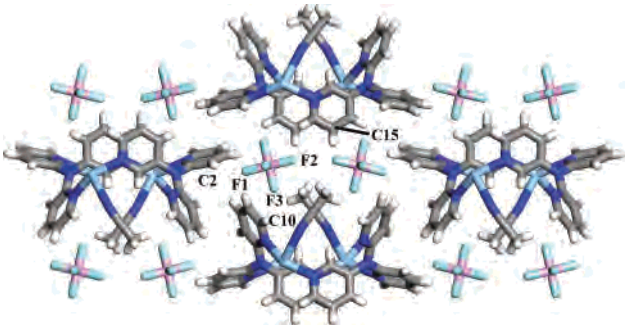

Figure 11. View down the chain axis of **4** showing interchain packing and hydrogen-bonding. Carbon, oxygen, and fluorine atoms involved in H-bonding interactions are labeled.

the much smaller size of acetonitrile compared to that of triflate. Compounds **4** and **5** form a ribbonlike 1D coordination polymer similar to that of **3**. However, in the structure of **3**, the triflate ligand is pointing outward from the 1D polymer while, in contrast, the CH_3CN ligands in **4** and **5** are all pointing inward to the 1D polymer (Figure 9), which can again be attributed to the size difference between the triflate and the CH_3CN ligands.

(c) π-Stacking Interactions. For a ligand with such a π-rich system as tpa, there are surprisingly few π-stacking interactions. The only interaction that can truly be considered a π-stack, between the pyridyl rings (N(1) ring) from two adjacent 1D strands, in **3**, is almost a textbook example[13] (Figure 10). The centroid−centroid distance between the pyridyl rings is 3.904 Å, which is slightly above the optimal distance for π-stacking, but the angle between the planes is 0°. There is also a horizontal slip of one-half of the ring, which is common to face-to-face π-stacking interactions.[13] There also appears to be a π-stack between the inner pyridyl rings in the dimer unit of **1**, but the centroid−centroid distance is 4.27 Å, and there is a horizontal slip of a full ring, making it unlikely that any real interaction exists.

(d) Other Weak Interactions. There are a number of πC−H···O interactions[15] in both compounds **2** and **3**. In **2**, there is a weak interaction between the nitrate O(2) and H(10) on one adjacent chain (C(10)−O(2) 3.739(6) Å, 129.4(3)°) and a slightly stronger interaction between the nitrate O(3) and the H(9) on the same adjacent chain (C(9)−O(3) 3.611(7) Å, 162.5(3)°). As well, there are interactions between the same nitrate O(3) and both H(4) and H(5) on a second adjacent chain (C(4)−O(3) 3.371(6) Å, 119.0(4)°; C(5)−O(3) 3.285(6) Å, 129.5(4)°), and H(14) on a third adjacent chain (C(14)−O(3) 3.288(5) Å, 141.7(3)°). There are also interactions between the nitrate O(1) and H(15) on a different pyridyl ring on the third adjacent chain (C(15)−O(1) 3.230(6) Å, 121.1(4)°). In compound **3**, there are weak interactions between the triflate O(2) and O(3) and H(8) on one adjacent chain (C(8)−O(2) 3.61(2) Å, 134.2(15)°; C(8)−O(3) 3.39(2) Å, 135.6(14)°) and between the triflate F(3) and H(2) on a second adjacent chain (C(2)−F(3) 3.597(18) Å, 135.7(12)°), as well as a stronger interaction between O(3) and H(3) on the second adjacent chain (C(3)−O(3) 3.34(2) Å, 174.8(15)°). Compound **4** exhibits a number of weak πC−H···F interactions, the strongest of which are between F(1) and H(2) (C(2)−F(1) 3.104(5) Å, 132.8(3)°), F(2) and H(15) (C(15)−F(2) 3.191(6) Å, 137.1(4)°), and F(3) and H(10) (C(10)−F(3) 3.417(6) Å, 138.0(3)°). Compound **5** displays only a few, weak πC−H···O interactions, but the distances and angles are not meaningful because of the disorder in the perchlorate anion. Figure 11 shows an example of the H-bonding interactions present in the complexes.

Luminescent Properties. All UV−vis absorption and luminescent spectra were recorded at a concentration of 1×10^{-4} M in acetonitrile, and data are summarized in Table 3. The room temperature UV−vis absorption and solution luminescence spectra of compounds **1**−**5** resemble those of the free tpa ligand (see Figure 12). The UV−vis absorption maxima are at 298 nm for tpa and for complexes **1**−**5**, and the molar extinction coefficients are in a similar range, indicating the absorption is a $\pi-\pi^*$ transition. The excitation maximum for tpa is at $\lambda = 316$ nm, and the maxima for compounds **1**−**5** are at $\lambda = 319$, 315, 318, 317, and 309 nm, respectively, while the emission maxima are at $\lambda = 361$, 366, 368, 367, 367, and 368 nm, for tpa and **1**−**5**, respectively. The NMR data for the complexes appear to indicate that compounds **1**−**5** undergo a dynamic exchange in solution as only one set of chemical shifts for the two 2-pyridyl groups (which are not equivalent in the crystal structures) was observed for all five compounds at ambient temperature. Low temperature ^{1}H NMR study in CD_3CN (compounds **1**−**5** are soluble only in acetonitrile) did not reveal the slow exchange region in the temperature range studied (233−298 K), although there was a change in the positions for some of the proton chemical shifts. The resemblance of the emission spectra of **1**−**5** with that of the free tpa supports that the luminescence of the complexes is tpa-based emission, which is fluorescent, caused by a $\pi^*-\pi$ transition, as evidenced by the molar extinction coefficients, lifetime measurements, and theoretical studies on related Zn(II) compounds.[7a] When the excitation and emission spectra are recorded in acetonitrile at 77 K, the difference between the free tpa and complexes **1**−**5** becomes more apparent (Figure 13). The excitation maxima at low temperature for **1**−**5** ($\lambda = 338$, 340, and 338 nm for **1**, **2**, and **3**, and 342 nm for **4** and **5**) are red-shifted by 19−33 nm as compared to the room temperature values, but the emission maxima are

(15) (a) Desiraju, G. R. *Acc. Chem. Res.* **1991**, *24*, 290. (b) Desiraju, G. R. *Acc. Chem. Res.* **1996**, *29*, 441. (c) Steiner, T.; Desiraju, G. R. *Chem. Commun.* **1998**, 891. (d) Steiner, T. *Chem. Commun.* **1997**, 727.

Table 3. UV−Vis and Luminescent Spectral Data for tpa and **1**−**5**, at 1×10^{-4} M in CH_3CN

cmpd	absorbance λ_{max}, nm	excitation λ_{max},[a] nm	emission λ_{max},[a] nm	ϵ, L/mol·cm	quantum yield[b]	lifetime, ms
			298 K			
tpa	298	316 (322)	361 (369)	15 800	0.383	
1	298	319 (380)	366 (471)	16 300	0.183	
2	298	315 (384)	368 (470)	11 700	0.165	
3	298	318 (373)	367 (452)	18 800	0.182	
4	298	317 (372)	367 (470)	16 800	0.165	
5	298	309 (381)	368 (470)	17 300	0.166	
			77 K			
tpa		333	432			0.00666 ± 0.00095
1		338	452			2.091 ± 0.036
2		340	453			2.706 ± 0.041
3		338	450			2.681 ± 0.048
4		342	450			2.466 ± 0.018
5		342	454			2.181 ± 0.027

[a] Numbers in parentheses are for the solid state. [b] With respect to 9,10-diphenylanthracene standard.

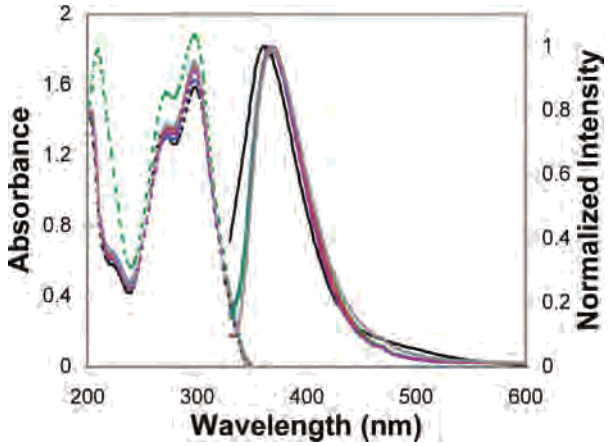

Figure 12. UV−visible absorption spectra (- - -) and emission spectra (—) at ambient temperature in CH_3CN (1×10^{-4} M) for tpa (black), **1** (blue), **2** (light blue), **3** (red), **4** (violet), and **5** (grey).

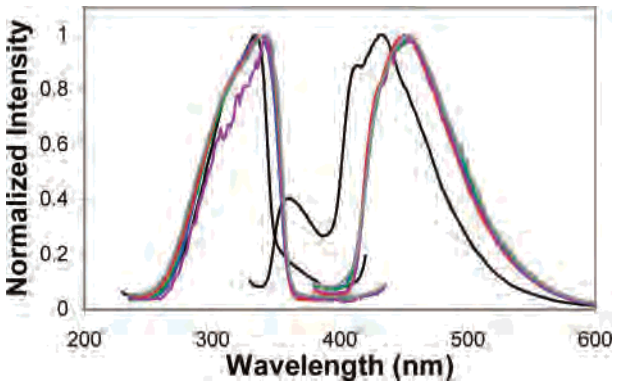

Figure 13. Excitation and emission spectra at 77 K in CH_3CN (1×10^{-4} M) for tpa (black), **1** (blue), **2** (light blue), **3** (red), **4** (violet), and **5** (grey).

red-shifted by 83−86 nm (λ = 452, 453, 450, 450, and 454 nm for **1**−**5**, respectively). The free tpa also shows a significant red-shift for both its excitation and emission maxima upon cooling to 77 K (ex λ_{max} = 333 nm, em λ_{max} = 432 nm), but there is still evidence of an emission peak at λ_{max} = 360 nm. At room temperature in the solid state, the emission maxima for the complexes are red-shifted even further, to λ_{max} = 471 and 452 nm for **1** and **3**, and 470 nm for **2**, **4**, and **5**, respectively, causing their greenish blue emission color, and therefore are not particularly useful for applications in electroluminescent devices. Quantum yield

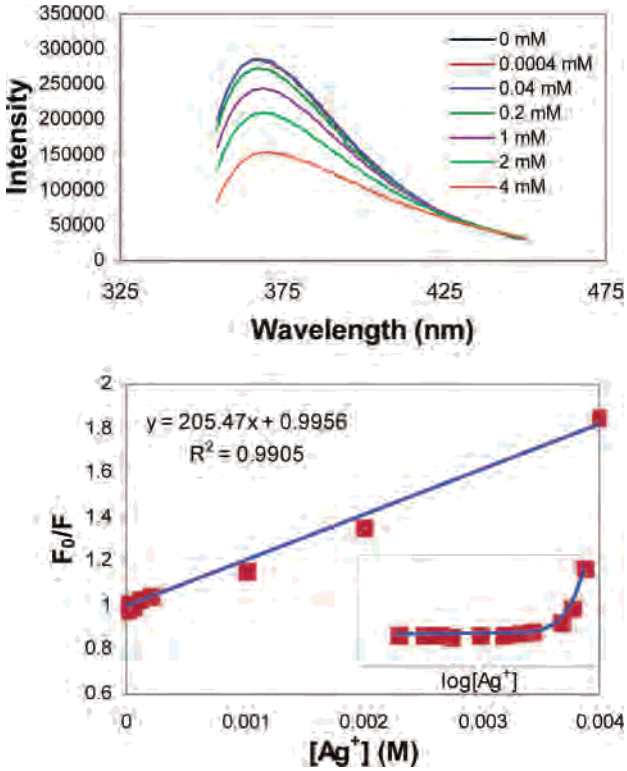

Figure 14. Top: emission curves of a 2 mM acetonitrile solution of tpa with varying concentrations of $AgNO_3$ added (shown in inset). Bottom: Stern−Volmer plot. Inset shows the same curve with Ag^+ concentration scaled logarithmically.

values for **1**−**5** range between 0.165 and 0.183, while the quantum yield for the free ligand is 0.383, relative to that of 9,10-diphenylanthracene. This indicates that, unlike Zn(II), the Ag(I) ion does negatively impact the luminescence of the tpa ligand. The luminescent lifetimes of **1**−**5** in CH_3CN glasses at 77 K are 2.09, 2.71, 2.68, 2.47, and 2.18 ms, respectively, indicating that these are all phosphorescent emissions. While the lifetime of the tpa emission peak at λ_{max} = 432 nm is 6.7 μs, indicating that it is likely a phosphorescent emission, the lifetime of the emission peak at λ_{max} = 360 nm was too fast to be measured on our spectrometer, indicating it is likely a fluorescent emission. It is likely that, at ambient temperatures, the thermal motion

and interaction with solvent molecules quench the phosphorescence; hence, only fluorescent emission is observed.

Using 2,2′,3″-tpa as a Fluorescent Sensor for Ag(I) Ions. Although the emission spectra of the silver(I) complexes **1**−**5** resemble that of the free 2,2′,3″-tpa ligand, we have observed that the presence of the Ag(I) ion in solution does cause a significant change in the emission intensity of the tpa ligand. In fact, the presence of any of the silver(I) salts used in our synthesis quenches the fluorescence of the tpa in solution, as seen by the difference in the quantum yields of the free ligand and complexes. This quenching can be attributed to the *heavy atom effect*[16] due to the coordination of the tpa ligand to the silver(I) center. The sensitivity of the fluorescence intensity of tpa toward Ag(I) ions made us interested in the possibility of using tpa as a luminescent sensor for Ag(I) ions. To establish the feasibility of tpa as a Ag(I) ion sensor, we examined the dependence of the emission intensity of tpa (2 mM solution in CH_3CN) on the concentration of Ag(I) ions. As shown by Figure 14, the intensity of the tpa emission decreases with increasing Ag(I) concentration. A Stern−Volmer plot of F_0/F versus ppm of Ag(I) shows a linear correlation, with a Stern−Volmer constant of 205.47 M^{-1}, and a correlation factor (R^2) of 0.990 (Figure 14). In contrast, when a similar trial was conducted for Zn(II) in the same concentration range, no apparent fluorescent quenching by the Zn(II) ion was observed, indicating that the 2,2′,3″-tpa ligand may be able to selectively detect Ag(I) ions. The structures displayed by compounds **1**−**5** represent possible modes of interactions between the tpa and the Ag(I) ion that lead to the fluorescence quenching.

(16) (a) Drago, R. S. *Physical Methods in Chemistry*; W. B. Saunders Company: Philadelphia, 1977; Chapter 5. (b) Masetti, F.; Mazzucato, U.; Galiazzo, G. *J. Lumin.* **1971**, *4*, 8. (c) Werner, T. C.; Hawkins, W.; Facci, J.; Torrisi, R.; Trembath, T. *J. Phys. Chem.* **1978**, *82*, 298.

Conclusions

We have demonstrated here that the 2,2′,3″-tpa ligand forms a variety of complexes with silver(I), whose structures depend greatly on the counterion used in the formation of the complex. The complexes **1**−**5** formed display blue luminescence, which is significantly red-shifted at low temperatures (77 K). The low temperature luminescence of the complexes is most likely phosphorescent in nature. Unlike the related Zn(II) complexes of 2,2′,3″-tpa where the tpa ligand functions as either a terminal ligand through the 3-pyridyl nitrogen atom or as a chelate ligand through the two 2-pyridyl groups, the Ag(I) complexes of tpa display the bridging modes only. The emission intensity of the tpa ligand is sensitive to the presence of Ag(I) ions, which may be useful for the detection of Ag(I) ions.

Acknowledgment. We thank the Natural Sciences and Engineering Council of Canada and the Xerox Research Foundation for financial support, and the Government of Ontario for an Ontario Graduate Scholarship (C.S.).

Supporting Information Available: Listings of X-ray experimental details, atomic coordinates, thermal parameters, and bond distances and angles (pdf), crystallographic information files (CIF), and figures showing extended solid-state packing and H-bonding interactions. This material is available free of charge via the Internet at http://pubs.acs.org.

IC020480Q